

# Electromagnetic Response of Static and Fluctuating Stripes in Cuprate Superconductors

M. Dumm\* and D. N. Basov

*Department of Physics, University of California at San Diego, La Jolla, California 92093-0319*

Seiki Komiya, Yasushi Abe, and Yoichi Ando

*Central Research Institute of Electric Power Industry, Tokyo, Japan*

(Received 24 August 2001; published 22 March 2002)

Using infrared spectroscopy, we found that changes in the in-plane charge dynamics attributable to static stripe order in  $\text{La}_{1.275}\text{Nd}_{0.6}\text{Sr}_{0.125}\text{CuO}_4$  or superconductivity in  $\text{La}_{1.875}\text{Sr}_{0.125}\text{CuO}_4$  are confined to energies smaller than  $100\text{ cm}^{-1}$ . An absorption peak in the low- $\omega$  conductivity of the Nd-doped compound is suggestive of localization effects due to the reduced dimensionality of static charge stripes. Neither superconductivity nor static stripe ordering has a noticeable effect on the depression of the scattering rate at  $\omega < 1000\text{ cm}^{-1}$  characteristic of the pseudogap state in other classes of moderately doped cuprates.

DOI: 10.1103/PhysRevLett.88.147003

PACS numbers: 74.25.Gz, 74.72.Dn

Upon doping with charge carriers a broad class of antiferromagnetic (AF) insulators reveals the astonishing phenomenon of high- $T_c$  superconductivity. Owing to the persistence of AF fluctuations, even in (heavily) doped phases the response of holes in cuprates is markedly different from free electron behavior. Specifically, the spectrum of both charge and spin excitations of moderately doped materials is characterized by a partial gap or pseudogap observed below  $T^* > T_c$  [1]. Moreover, many cuprates show a remarkable tendency towards segregation of doped charges into one-dimensional (1D) self-organized regions (stripes) within the two-dimensional (2D)  $\text{CuO}_2$  planes [2,3]. At least within some models, stripe fluctuations are believed to play a pivotal role in the development of the pseudogap and have been proposed to be the driving force for high- $T_c$  superconductivity [4,5]. Although the evidence for the existence of stripes (static or fluctuating) in a variety of cuprates is overwhelming [6–9] their role in carrier dynamics is yet to be systematically investigated. The interplay between the stripes physics and the formation of the pseudogap or superconducting gap also remains unclear. In order to address these issues we employed infrared spectroscopy to examine the way in which the stripe environment impedes on the dynamics of doped holes in the  $\text{CuO}_2$  planes.

In this Letter we report on the dynamical conductivity of  $\text{La}_{1.875}\text{Sr}_{0.125}\text{CuO}_4$  (LSCO) and  $\text{La}_{1.275}\text{Nd}_{0.6}\text{Sr}_{0.125}\text{CuO}_4$  (LNSCO). The former system is a high- $T_c$  superconductor with  $T_c = 32\text{ K}$ . Although there are strong indications for fluctuating stripes in  $\text{La}_{2-x}\text{Sr}_x\text{CuO}_4$ , for  $x = 1/8$  static AF correlations do not occur at  $T > T_c$  [10]. The Nd-doped system is a nonsuperconducting counterpart of LSCO; static charge-stripe ordering occurs below the structural phase transition from the low-temperature orthorhombic (LTO) to the low-temperature tetragonal (LTT) phase at  $T_{d_2} \approx 80\text{ K}$  [6]. The broad spectral coverage of our experiments spanning from sub-THz frequencies to UV light provides access to all relevant energy scales in

the studied systems, including localization, superconducting gap, pseudogap, and others.

High-quality single crystals were grown by the traveling-solvent floating-zone technique. The samples were well characterized by x-ray and dc resistivity measurements [11] (see the inset of Fig. 2). We obtained the complex conductivity  $\sigma = \sigma_1 + i\sigma_2$  from the frequency dependent reflectivity  $R(\omega)$  using Kramers-Kronig analysis. Our measurements were carried out at frequencies from  $15$  to  $48\,000\text{ cm}^{-1}$  ( $2\text{ meV}$ – $6\text{ eV}$ ) and at temperatures from  $5$  to  $293\text{ K}$ . After a first run, the disk shaped crystals with diameter  $d \approx 5\text{ mm}$  were coated *in situ* with gold or aluminum in the cryostat. The metal-coated samples were measured as the reference in a second run [12]. For the low- $\omega$  extrapolation we used resistivity data; for the high frequency extrapolation we utilized the data published by Uchida *et al.* [13] for Nd-free LSCO.

In Fig. 1,  $\sigma_1(\omega)$  of  $\text{La}_{1.875}\text{Sr}_{0.125}\text{CuO}_4$  and  $\text{La}_{1.275}\text{Nd}_{0.6}\text{Sr}_{0.125}\text{CuO}_4$  are plotted at various temperatures. For  $\omega \geq 1000\text{ cm}^{-1}$   $\sigma_1(\omega)$  is only weakly temperature dependent with nearly the same absolute value in both compounds. When integrated up to  $10\,000\text{ cm}^{-1}$ , the effective spectral weight  $N_{\text{eff}}(\omega) = \int_0^\omega \sigma_1(\omega') d\omega'$  is the same for Nd-doped and Nd-free LSCO for all temperatures investigated within an error margin of 5%. This result is in fair agreement with results obtained on  $\text{La}_{1.6-x}\text{Nd}_{0.4}\text{Sr}_x\text{CuO}_4$  for  $x = 0.1$  and  $0.15$  [14]. However, our measurements do not confirm the substantial suppression of spectral weight found in  $\text{La}_{1.48}\text{Nd}_{0.4}\text{Sr}_{0.12}\text{CuO}_4$  up to  $8000\text{ cm}^{-1}$  [14].

It is obvious that Nd doping has no impact on the conductivity spectrum above  $1000\text{ cm}^{-1}$  even below  $T_{d_2}$ . This result departs from the behavior expected in a system with static stripe order. Theoretical calculation on clusters of charge stripes predict that most of the electronic spectral weight is shifted from a Drude channel at  $\omega = 0$  to a mode at  $\omega \approx 0.35\text{ eV}$  ( $3000\text{ cm}^{-1}$ ) [15]. Such a shift is not detected in our data. Apart from this, interactions

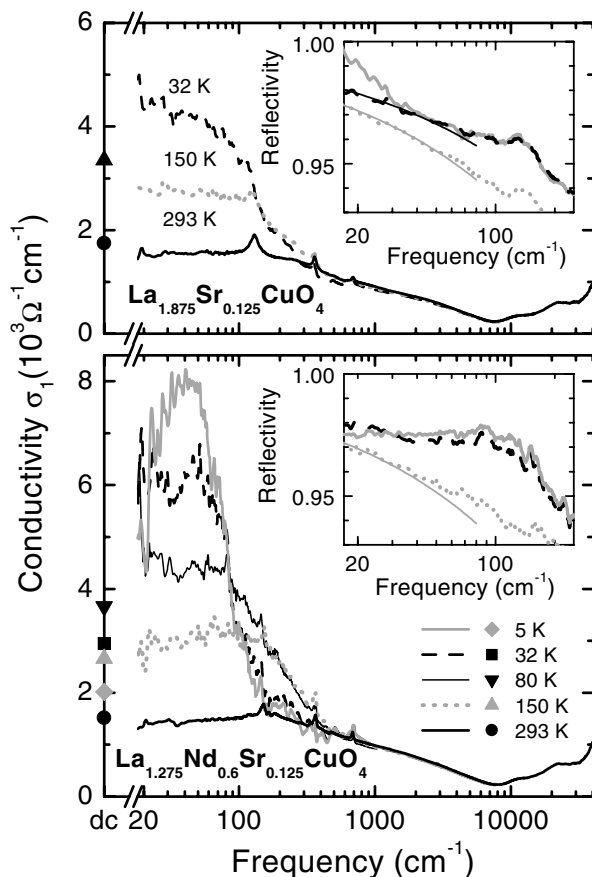


FIG. 1. Frequency dependence of the real part of the in-plane conductivity  $\sigma_1(\omega)$  of LSCO and LNSCO. The symbols on the left ordinates represent the in-plane dc conductivity  $\sigma_{dc}$ . The insets show the reflectivity spectra of both cuprates at 150, 32, and 5 K for  $\omega \leq 250 \text{ cm}^{-1}$ . The thin solid lines are calculated with the Hagen-Rubens formula using the actual  $\sigma_{dc}$  values.

between 1D charge channels usually drive a phase transition to a charge-density-wave (CDW) ground state as observed in quasi-1D organic conductors [16]. In insulating static stripe ordered nickelate  $\text{La}_{2-x}\text{Sr}_x\text{NiO}_4$  a temperature dependent charge gap  $2\Delta \approx 0.26 \text{ eV}$  opens in  $\sigma_1(\omega)$  below the charge-stripe ordering transition [17]. No signatures of a charge gap are observed in LNSCO below  $T_{d2}$ .

Our results indicate that the static stripe order in LNSCO below  $T_{d2}$  is different from the idealized picture of static 1D “rivers of charges” separated by insulating AF domains. This is in accord with several theoretical studies of the stripe ordered phase in cuprates. For example, it has been suggested that the formation of a CDW along the stripes can be suppressed by disorder in the coupling between the stripes or by transverse fluctuations of the stripes [5,18]. Additionally, calculations within the  $t$ - $J$  model showed that stripes have a width of several lattice spacings which results in a finite overlap at  $x = 1/8$  doping [19]. This picture of a more or less “imperfect” stripe order in  $\text{La}_{2-x-y}\text{Nd}_y\text{Sr}_x\text{CuO}_4$  is in agreement with recent results from neutron-scattering and angle-resolved photoemission experiments. [9,20].

Below  $1000 \text{ cm}^{-1}$ , the optical conductivity is strongly temperature dependent. In LSCO  $\sigma_1(\omega)$  increases monotonically with decreasing temperatures and frequencies for  $T > T_c$ . LNSCO shows a completely different frequency dependence of  $\sigma_1(\omega)$ : as seen in the lower panel of Fig. 1, a peak feature centered at finite frequencies continuously develops in the conductivity spectrum when the sample is cooled down. Dc conductivity data plotted as symbols on the ordinate indicate that this nonmonotonic behavior of  $\sigma_1(\omega)$  already exists at temperatures above  $T_{d2} \approx 80 \text{ K}$ . As temperature is reduced, the peak narrows and seems to shift towards lower frequencies. A comparison between the measured  $R(\omega)$  data and the values calculated with the Hagen-Rubens formula in the inset of Fig. 1 confirms metallic behavior in LSCO above  $T_c$ . In contrast, there are already deviations from the calculated  $R(\omega)$  at 150 K in LNSCO. Despite the fact that  $\sigma_{dc,5 \text{ K}} < \sigma_{dc,150 \text{ K}}$  the reflectivity increases further with decreasing temperature, especially in the region around  $100 \text{ cm}^{-1}$ . It is obvious that the peak in  $\sigma_1(\omega)$  at low temperatures originates from this strong enhancement of  $R(\omega)$  over the Hagen-Rubens value.

It has been shown that a peak in  $\sigma_1(\omega)$  can be initiated by disorder in the  $\text{CuO}_2$  planes and may result from localization of charge carriers [21,22]. A conductivity peak at finite frequencies seems to be a generic feature of low-dimensional disordered conductors near the metal-insulator transition [23,24]. Another signature of localization in LNSCO is the upturn in the resistivity below  $T_{d2}$  (see the inset of Fig. 2). In contrast, no signs of localization are observed in LSCO: there is no peak in  $\sigma_1(\omega)$  and the dc transport is metallic above  $T_c$ . Notably, the Nd dopant in LNSCO is neutral since both La and Nd are trivalent. Therefore disorder potential associated with Nd is less prominent than that induced by either charged impurities such as O or Sr [25] or by direct substitution of Cu in the  $\text{CuO}_2$  planes with other elements. But the introduction of Nd rotates the direction of distortion in the  $\text{CuO}_2$  planes from diagonal to parallel to the Cu-O bond [27] which supports the pinning of stripes below  $T_{d2}$  [6] and therefore changes the environment in which mobile charge carriers move. Hence, the localization peak in  $\sigma_1(\omega)$  at finite frequencies is consistent with the idea of the reduced dimensionality of LNSCO compared to LSCO. Indeed, if fluctuating stripes become pinned by lattice distortions the charge carriers are confined to (quasi) 1D static stripes and are more susceptible to localization due to disorder. The continuous development of the conductivity peak through  $T_{d2}$  is consistent with recent results from x-ray- and neutron-scattering experiments on  $\text{La}_{1.6-x}\text{Nd}_{0.4}\text{Sr}_x\text{CuO}_4$ . These studies showed that some fraction of LTT-like domains persist in the LTO phase above  $T_{d2}$  [20,28].

For further discussion of the charge dynamics it is useful to introduce the frequency dependent scattering rate  $1/\tau(\omega)$ . In the framework of the extended

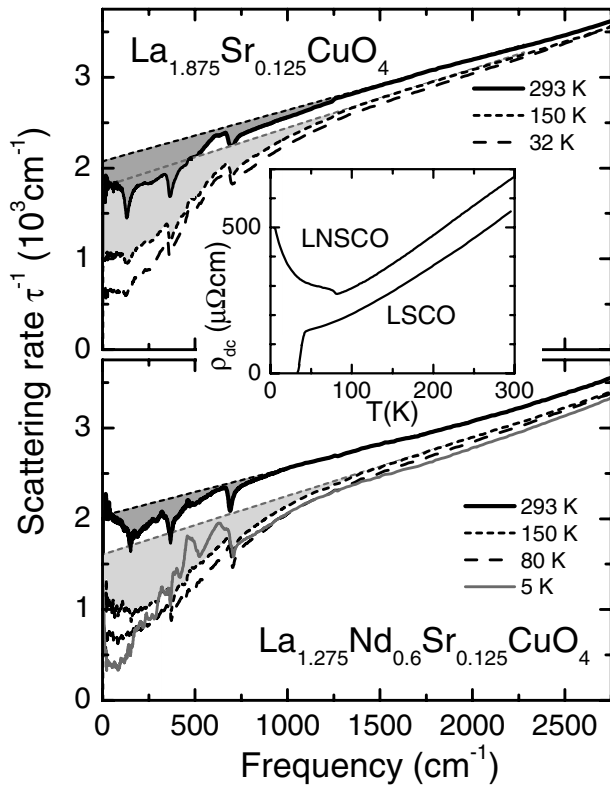


FIG. 2. Frequency dependence of the in-plane scattering rate  $1/\tau(\omega)$  of LSCO and LNSCO. The thin dashed lines represent a low- $\omega$  extension of the linear frequency dependence observed at high  $\omega$ . The shaded areas indicate the suppression of  $1/\tau(\omega)$  in the pseudogap regime for 293 and 150 K. The inset shows the dc in-plane resistivities. The step in  $\rho_{dc}$  of LNSCO occurs at the structural phase transition.

Drude model the optical constant  $1/\tau(\omega)$  is defined as  $4\pi/\tau(\omega) = \omega_p^2 \sigma_1(\omega)/[\sigma_1^2(\omega) + \sigma_2^2(\omega)]$ . The plasma frequency  $\omega_p$  is obtained by integrating  $\sigma_1(\omega)$  up to the onset frequency of interband absorption [29]. Figure 2 shows  $1/\tau(\omega)$  of LSCO and LNSCO. At high frequencies the scattering rate increases linearly with frequency for all temperatures in both materials. In contrast,  $1/\tau(\omega)$  decreases much faster than linear for  $\omega \leq 1000 \text{ cm}^{-1}$ . This behavior is a characteristic signature of charge dynamics in the pseudogap state below  $T^*$  [1,30]. The depression of the scattering rate is observed in the whole temperature range investigated indicating that  $T^*$  exceeds room temperature in both compounds. It is obvious that Nd doping and static stripe ordering has only a little influence on the suppression of  $1/\tau(\omega)$  below  $1000 \text{ cm}^{-1}$ . Compared to the other cuprates, the onset of the pseudogap behavior is somewhat smoother and shifted towards higher energies.

In Fig. 3 we focus on the charge dynamics of LSCO at low temperatures and frequencies. For  $T < T_c$  and  $\omega < 100 \text{ cm}^{-1}$ ,  $\sigma_1(\omega)$  decreases below the normal state values as indicated by the shaded area in the upper panel. This is reminiscent of the loss of spectral weight in  $\sigma_1(\omega)$  below  $T_c$  due to formation of the superconducting gap in

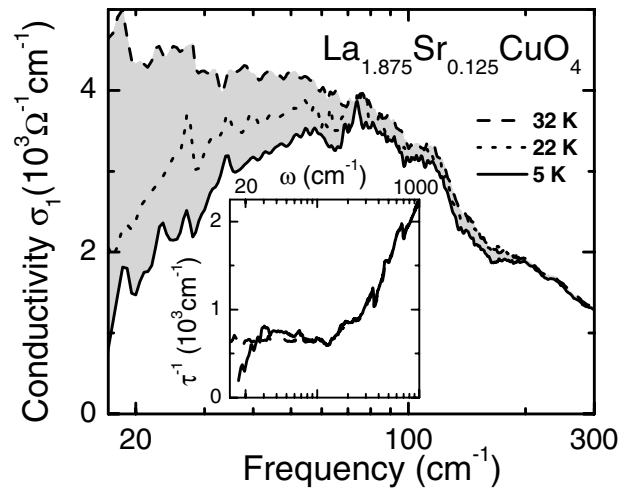


FIG. 3. Real part of the in-plane conductivity and scattering rate (inset) of LSCO at  $T \leq T_c$ . The shaded area quantifies the spectral weight of the superconducting condensate at 5 K.

$\text{La}_{2-x}\text{Sr}_x\text{CuO}_4$  with  $x = 0.15$  [31] or  $0.17$  [32]. To check if the missing spectral weight in  $\sigma_1(\omega)$  can be attributed to superconductivity, we calculated the in-plane penetration depth  $\lambda_{ab}$  in two different ways: from the imaginary part of the conductivity  $c^2/\lambda_{ab}^2 = 4\pi\omega\sigma_2(\omega)$  and by applying the Ferrell-Glover-Tinkham sum rule  $c^2/\lambda_{ab}^2 = 8 \int_0^\infty (\sigma_n - \sigma_s) d\omega$ , where  $\sigma_n$  and  $\sigma_s$  are the real parts of the conductivity at 32 K and below  $T_c$ , respectively [33]. The results we obtained from both calculations agree very well. At 5 K,  $\lambda_{ab} \approx 630 \text{ nm}$  which is consistent with the results from microwave measurements [34]. Therefore, the decrease of  $\sigma_1(\omega)$  at an energy scale  $\omega < 100 \text{ cm}^{-1}$  can be attributed to the formation of the superconducting condensate.

The lower panel of Fig. 3 shows  $1/\tau(\omega)$  at 5 K and at  $T_c$ . In the superconducting state,  $1/\tau(\omega)$  first increases below  $100 \text{ cm}^{-1}$  and then decreases at the very low-frequency end while it is frequency independent in the normal state. In contrast, no change in the scattering rate is observed at the superconducting transition in the frequency region between 100 and  $1000 \text{ cm}^{-1}$  where the form of the  $1/\tau(\omega)$  spectrum is dominated by the pseudogap. Thus, superconductivity has no impact on the charge dynamics in this energy range indicating that pseudogap and superconducting gap have different origins. Consistent with this view is the fact that in LSCO the characteristic temperatures and the energy scales of pseudogap and superconducting gap differ by about 1 order of magnitude [35] (Figs. 2 and 3). Notably, the pseudogap behavior is not affected by Nd doping while superconductivity is totally suppressed. This latter result along with the energy scales discrepancy discussed above argues against the decisive role of superconducting fluctuations in the development of the pseudogap. Our finding is in agreement with tunneling experiments [37] and infrared studies of the electron doped cuprates [38].

If we compare  $\sigma_1(\omega)$  of Nd-doped LSCO plotted in the lower panel of Fig. 1 with  $\sigma_1(\omega)$  of LSCO (upper panel of Fig. 3) it appears that the energy scale of the localization peak in LNSCO is of a similar order of magnitude as the superconducting gap in LSCO. It has been shown that in Zn-doped  $\text{YBa}_2\text{Cu}_4\text{O}_8$  crystals the spectral weight confined under the localization peak in  $\sigma(\omega, T > T_c)$  is excluded from contributing to the superconducting condensate at  $T < T_c$  [22]. Thus the destructive role of charge localization for superconductivity in static stripe ordered Nd-doped LSCO is especially prominent because the superconducting gap in Nd-free LSCO is anomalously small.

In summary, we observed a finite-frequency peak in the far-infrared conductivity of LNSCO that can be attributed to localization of charge carriers in the  $\text{CuO}_2$  planes. This result is consistent with the reduced dimensionality of the electronic transport in the static stripe ordered state. Apart from these localization effects the overall electromagnetic response of both static and fluctuating stripes is similar indicating that “static” stripe order in LNSCO deviates from the idealized picture of 1D charge channels insulated by AF domains. Although the impact of static stripes is confined to very low frequencies, the energy scale attributable to localization appears to be comparable to the magnitude of the superconducting gap in LSCO. Neither static stripe ordering in LNSCO nor superconductivity in LSCO has an influence on the pseudogap behavior observed at much higher temperature and energy scales.

This research was supported by the U.S. Department of Energy Grant No. DE-FG03-00ER45799.

\*Present address: 1. Physikalisches Institut, Universität Stuttgart, 70550 Stuttgart, Germany.

Email address: dumm@pi1.physik.uni-stuttgart.de

- [1] T. Timusk and B. Statt, Rep. Prog. Phys. **62**, 61 (1999).  
 [2] J. Zaanen and O. Gunnarsson, Phys. Rev. B **40**, 7391 (1989); H.J. Schulz, Phys. Rev. Lett. **64**, 1445 (1990); M. Cato and K. Machida, J. Phys. Soc. Jpn. **59**, 1047 (1990); J. Zaanen, Science **286**, 251 (1999).  
 [3] J. Orenstein and A.J. Millis, Science **288**, 468 (2000).  
 [4] V.J. Emery and S.A. Kivelson, Nature (London) **374**, 434 (1995).  
 [5] V.J. Emery, S.A. Kivelson, and O. Zachar, Phys. Rev. B **56**, 6120 (1997).  
 [6] J.M. Tranquada *et al.*, Nature (London) **375**, 561 (1995).  
 [7] J.M. Tranquada *et al.*, Phys. Rev. B **54**, 7489 (1996); M.v. Zimmermann *et al.*, Europhys. Lett. **41**, 629 (1998); K. Yamada *et al.*, Phys. Rev. B **57**, 6165 (1998); Y. Ando, A.N. Lavrov, and K. Segawa, Phys. Rev. Lett. **83**, 2813 (1999); Y. Ando *et al.*, cond-mat/0108053; A.W. Hunt *et al.*, Phys. Rev. Lett. **82**, 4300 (1999).  
 [8] T. Noda, H. Eisaki, and S. Uchida, Science **286**, 265 (1999); X.J. Zhou *et al.*, Science **286**, 268 (1999).  
 [9] X.J. Zhou *et al.*, Phys. Rev. Lett. **86**, 5578 (2001).  
 [10] T. Suzuki *et al.*, Phys. Rev. B **57**, R3229 (1998); H. Kimura *et al.*, *ibid.* **59**, 6517 (1999).  
 [11] Y. Ando *et al.*, Phys. Rev. Lett. **87**, 017001 (2001).  
 [12] C.C. Homes *et al.*, Appl. Opt. **32**, 2976 (1993); this procedure reduces the uncertainty in  $R(\omega)$  to 0.3%.  
 [13] S. Uchida *et al.*, Phys. Rev. B **43**, 7942 (1991).  
 [14] S. Tajima *et al.*, Europhys. Lett. **47**, 715 (1999); Physica (Amsterdam) **341C–348C**, 1723 (2000).  
 [15] M.I. Salkola, V.J. Emery, and S.A. Kivelson, Phys. Rev. Lett. **77**, 155 (1996); T. Tohyama *et al.*, Phys. Rev. Lett. **82**, 4910 (1999); Y. Shibata, T. Tohyama, and S. Maekawa, Phys. Rev. B **64**, 054519 (2001).  
 [16] *Highly Conducting One-Dimensional Solids*, edited by J.T. Devreese, R.P. Evrard, and V.E. van Doren (Plenum, New York, 1979).  
 [17] T. Katsufuji *et al.*, Phys. Rev. B **54**, R14 230 (1996).  
 [18] S.A. Kivelson, E. Fradkin, and V.J. Emery, Nature (London) **393**, 550 (1998).  
 [19] S.R. White and D.J. Scalapino, Phys. Rev. Lett. **81**, 3227 (1998); A.L. Chernyshev, A.H. Castro Neto, and A.R. Bishop, *ibid.* **84**, 4922 (2000).  
 [20] J.M. Tranquada, N. Ichikawa, and S. Uchida, Phys. Rev. B **59**, 14 712 (1999).  
 [21] D.N. Basov *et al.*, Phys. Rev. B **49**, 12 165 (1994).  
 [22] D.N. Basov, B. Dabrowski, and T. Timusk, Phys. Rev. Lett. **81**, 2132 (1998).  
 [23] W. Götze and P. Wölfle, Phys. Rev. B **6**, 1226 (1972); K. Lee *et al.*, *ibid.* **52**, 4779 (1995).  
 [24] T. Osafune *et al.*, Phys. Rev. Lett. **82**, 1313 (1999).  
 [25] It has been shown by nuclear quadrupole resonance that the fraction of holes pinned in the  $\text{CuO}_2$  planes by charged dopants such as Sr or O increases with the effective charge of these dopants [26].  
 [26] P.C. Hammel *et al.*, Phys. Rev. B **57**, R712 (1998).  
 [27] M.K. Crawford *et al.*, Phys. Rev. B **44**, 7749 (1991).  
 [28] A.R. Moodenbaugh *et al.*, Phys. Rev. B **58**, 9549 (1998).  
 [29]  $\omega_p \approx 13\,000\text{ cm}^{-1}$  for both compounds with the integration limit of  $\omega = 7700\text{ cm}^{-1}$ .  
 [30] D.N. Basov *et al.*, Phys. Rev. Lett. **77**, 4090 (1996); A.V. Puchkov *et al.*, J. Phys. Condens. Matter **8**, 10 049 (1996); T. Startseva *et al.*, Phys. Rev. B **59**, 7184 (1999).  
 [31] H.S. Somal *et al.*, Phys. Rev. Lett. **76**, 1525 (1996).  
 [32] F. Gao *et al.*, Phys. Rev. B **47**, 1036 (1993).  
 [33] The first equation is a consequence of the presence of a  $\delta$  peak at  $\omega = 0$ ; the sum rule states that the missing spectral weight in  $\sigma_1(\omega)$  is transferred to the  $\delta$  function.  
 [34] T. Shibauchi *et al.*, Phys. Rev. Lett. **72**, 2263 (1994).  
 [35] Optical data on  $\text{YBa}_2\text{Cu}_3\text{O}_{6+\delta}$  and  $\text{Bi}_2\text{Sr}_2\text{CaCu}_2\text{O}_{8+\delta}$  [30,36] indicated that both gaps have comparable energy scales in these double layer cuprates.  
 [36] A.V. Puchkov *et al.*, Phys. Rev. Lett. **77**, 3212 (1996).  
 [37] V.M. Krasnov *et al.*, Phys. Rev. Lett. **84**, 5860 (2000); M. Suzuki and T. Watanabe, *ibid.* **85**, 4787 (2000).  
 [38] E.J. Singley *et al.*, Phys. Rev. B **64**, 224503 (2001).